frontiers in Marine Science

ORIGINAL RESEARCH
published: 11 January 2021
doi: 10.3389/fmars.2020.542386

Vertical Migration of Pelagic and Mesopelagic Scatterers From ADCP Backscatter Data in the Southern Norwegian Sea

Boris Cisewski[1], Hjálmar Hátún[2], Inga Kristiansen[2], Bogi Hansen[2], Karin Margretha H. Larsen[2], Sólvá Káradóttir Eliasen[2] and Jan Arge Jacobsen[2]*

[1] Thünen-Institut für Seefischerei, Bremerhaven, Germany, [2] Faroe Marine Research Institute, Tórshavn, Faroe Islands

Records of backscatter and vertical velocity obtained from moored Acoustic Doppler Current Profilers (ADCP) enabled new insights into the dynamics of deep scattering layers (DSLs) and diel vertical migration (DVM) of mesopelagic biomass between these deep layers and the near-surface photic zone in the southern Norwegian Sea. The DSL exhibits characteristic vertical movement on inter-monthly time scales, which is associated with undulations of the main pycnocline between the warm Atlantic water and the underlying colder water masses. Timing of the DVM is closely linked to the day-night light cycle—decent from the photic zone just before sunrise and ascent immediately after sunset. Seasonal variations are also evident, with the highest DVM activity and lowest depth averaged mean volume backscatter strength (MVBS) during spring. This suggests that both oceanographic and optical conditions are driving the complex dynamics of pelagic and mesopelagic activity in this region. We hypothesize that the increased abundance of calanoid copepods in the near-surface layer during spring increases the motivation for vertical migration of pelagic and mesopelagic species, which therefore can explain the increased DVM activity during this season.

Keywords: diel vertical migration, ADCP backscatter, seasonal cycles, deep scattering layer, Southern Norwegian Sea, mesopelagic fish, zooplankton

OPEN ACCESS

Edited by:
Ana M. Queiros, Plymouth Marine Laboratory, United Kingdom

Reviewed by:
Stein Kaartvedt, University of Oslo, Norway
Thor Aleksander Klevjer, Norwegian Institute of Marine Research (IMR), Norway

****Correspondence:***
Boris Cisewski
boris.cisewski@thuenen.de

Specialty section:
This article was submitted to Marine Ecosystem Ecology, a section of the journal Frontiers in Marine Science

Received: *15 April 2020*
Accepted: *09 December 2020*
Published: *11 January 2021*

Citation:
Cisewski B, Hátún H, Kristiansen I, Hansen B, Larsen KMH, Eliasen SK and Jacobsen JA (2021) Vertical Migration of Pelagic and Mesopelagic Scatterers From ADCP Backscatter Data in the Southern Norwegian Sea. Front. Mar. Sci. 7:542386. doi: 10.3389/fmars.2020.542386

INTRODUCTION

A widespread characteristic behavioral pattern of a variety of marine species, including zooplankton, mesopelagic micronekton and planktivorous and piscivorous fish, is their diel vertical migration (DVM) and subsequent distributional change over 24 h (Neilson and Perry, 1990). This DVM, conducted by marine taxa in the epipelagic (0–200 m) and the mesopelagic (200–1,000 m) zones in the ocean (Sutton, 2013; Klevjer et al., 2016) is potentially the largest animal migration on Earth in terms of biomass (Hays, 2003). The global occurrence of DVM impacts the ecosystem of the upper seas, altering habits of feeding, predation and ecological interactions (Bianchi et al., 2013). Aggregations of marine species are often detected in echo-sounders as shallow scattering layers and/or 'deep scattering layers' (DSLs) in the mesopelagic region, which can be seen rising around dusk and descending around dawn (Hays, 2003). Sound scattering layers are vertically narrow (tens to hundreds of m), but horizontally extensive (tens to thousands of km) structures comprising aggregations of zooplankton and mesopelagic fish in the water column

(Proud et al., 2017). In addition, the vertical migration of zooplankton and nekton plays an important part in the biological pump of the World Ocean, where atmospheric CO_2 is transferred as biogenic carbon to large depths (Longhurst and Harrison, 1988; Jónasdóttir et al., 2015; Turner, 2015). The migrating zooplankton and nekton feed in the epipelagic zone during night and return to the meso- or bathypelagic zone during day, thereby increasing the carbon flux to the deeper layers by excretion, fecal pellet production and mortality at depth (Bianchi et al., 2013). The necessity of understanding magnitude and patterns of the vertical migrations has recently become pressing. This is mainly due to realization that active carbon transport which is mediated by zooplankton and nekton vertical migrations has to be parameterized in global biogeochemical models (Bianchi et al., 2013).

While the evolutionary drivers of DVM and its influencing cues are not clearly understood (Lampert, 1989; Cohen and Forward, 2009), predator avoidance is generally considered to be the most likely underlying mechanism. Nocturnal upward migration may allow bathy- or mesopelagic species to feed in the epipelagic zone, and thereby reduce the risk of exposure to visually orientated predators during the day (Zaret and Suffern, 1976; Lampert, 1989). DVM is regarded as a behavioral response toward a combined set of exogenous environmental cues (Forward, 1988), where daylight seems the most important control. Several zooplankton studies conducted in freshwater and marine environments have shown that the migration times typically correspond to the times of rapid light intensity changes underwater around dusk and dawn (see Roe, 1974; Forward, 1988; Haney, 1988; Ringelberg, 1995).

In this study, we focus on the southern Norwegian Sea, which is dominated by warm and saline Modified North Atlantic Water (MNAW) entering the area from southwest, and cold and less saline East Icelandic Water (EIW) flowing from the northwest (**Figure 1A**). After crossing the Iceland-Faroe Ridge, the MNAW continues in a narrow boundary current, the Faroe Current, which flows eastward north of the Faroe Islands (Hansen et al., 2003, 2010; Hátún et al., 2004). The East Icelandic Current transports the EIW southeastwards where it meets the warmer and more saline MNAW in the southwestern Norwegian Sea. A sharp thermo/halocline, hereafter referred to as *the interface*, separates these two water masses (**Figure 1B**), and its vertical position changes on weekly to interannual, time scales (Hátún et al., In Prep; Hansen et al., 2019). This interface outcrops at the surface as the Iceland-Faroe Front (**Figure 1A**). We follow the water mass classification proposed by Read and Pollard (1992). North of the front, the uppermost 700 m are occupied by colder and less saline Norwegian North Atlantic Water (NNAW) and Norwegian Sea Arctic Intermediate Water (NSAIW) (**Figure 1B**).

The Norwegian Sea is highly productive and ecologically very important for large pelagic fish stocks such as Norwegian spring-spawning herring (*Clupea harengus*), Atlantic mackerel (*Scomber scombrus*), and blue whiting (*Micromesistius poutassou*) (Prokopchuk and Sentyabov, 2006). These fish stocks prey on the large biomasses of zooplankton, predominately the herbivore copepods *Calanus finmarchicus* and *C. hyperboreus* (Wiborg, 1955; Broms et al., 2009), omnivore euphausiids (*Meganyctiphanes norvegica* and *Thysanoessa* spp.), and carnivore amphipods (*Themisto* spp.). In addition, mesopelagic fish species such as *Maurolicus muelleri*, *Benthosema glaciale*, mesopelagic shrimps and jellyfish occupy the mesopelagic realm of these waters (Skjoldal, 2004)—acoustically identifiable as DSLs (Melle et al., 1993; Torgersen et al., 1997; Knutsen and Serigstad, 2001).

In 1988, the Faroe Marine Research Institute (FAMRI) started a monitoring program focusing on the state of the pelagic ecosystem north of the Faroe Islands in the southern Norwegian Sea, along the so-called Section N (**Figure 1**). In this monitoring program, a number of different biological and physical parameters have been collected. These include predominantly (1) velocity data and backscatter strength recorded with self-contained Acoustic Doppler Current Profilers (ADCPs), (2) measurements of the hydrography, (3) vessel-mounted echo-sounder data, and (4) accompanying zooplankton net hauls. ADCPs can complement conventional net sampling due to their advantages of operating autonomously throughout the year without being subject to the issue of avoidance, thereby providing sufficient resolution in depth and time for reliable inference of relevant DVM characteristics (Hovekamp, 1989; Zhou et al., 1994; Burd and Thomson, 2012). The drawback, however, is the reduced ability of species identification and the quantification of their abundances and biomass.

While most previous long-term studies of vertical migration patterns in the Norwegian Sea have been restricted to the Norwegian fjord system (e.g., Staby et al., 2011, 2013; Dypvik et al., 2012), we here present results of a long-term study conducted in the southern Norwegian Sea. Since vertical migration occurs on diel, seasonal and inter-annual time scales, long-term ADCP time series enable an analysis of the characteristic patterns of vertical migration over the entire temporal range. Based on two 1 year records of data retrieved from a self-contained ADCP moored near the core of the Faroe Current on section N from June 2013–May 2015 (**Figure 1**), we present the seasonal variation of the vertical velocity and the mean volume backscattering strength (MVBS) at a 20 min resolution. These provide accurate qualitative and quantitative information on the vertical migration patterns of mesopelagic species in a highly productive part of the Northeast Atlantic. Overall, the aims of this study are (1) the identification of DSL and DVM patterns and their seasonal variations and (2) the investigation of environmental conditions and cues controlling the vertical and temporal distribution of pelagic and mesopelagic species.

MATERIALS AND METHODS

Study Area

Standard Section N is comprised of 14 stations, labeled N01-N14, that extend northwards from the Faroe Islands and into the Norwegian Sea (**Figures 1A,B**). The stations are located from 62.33°N to 64.5°N at longitude 6.08°W, except for station N14 which is located at longitude 6.00°W. Since 1988, there have been up to four hydrographic cruises each year covering this standard

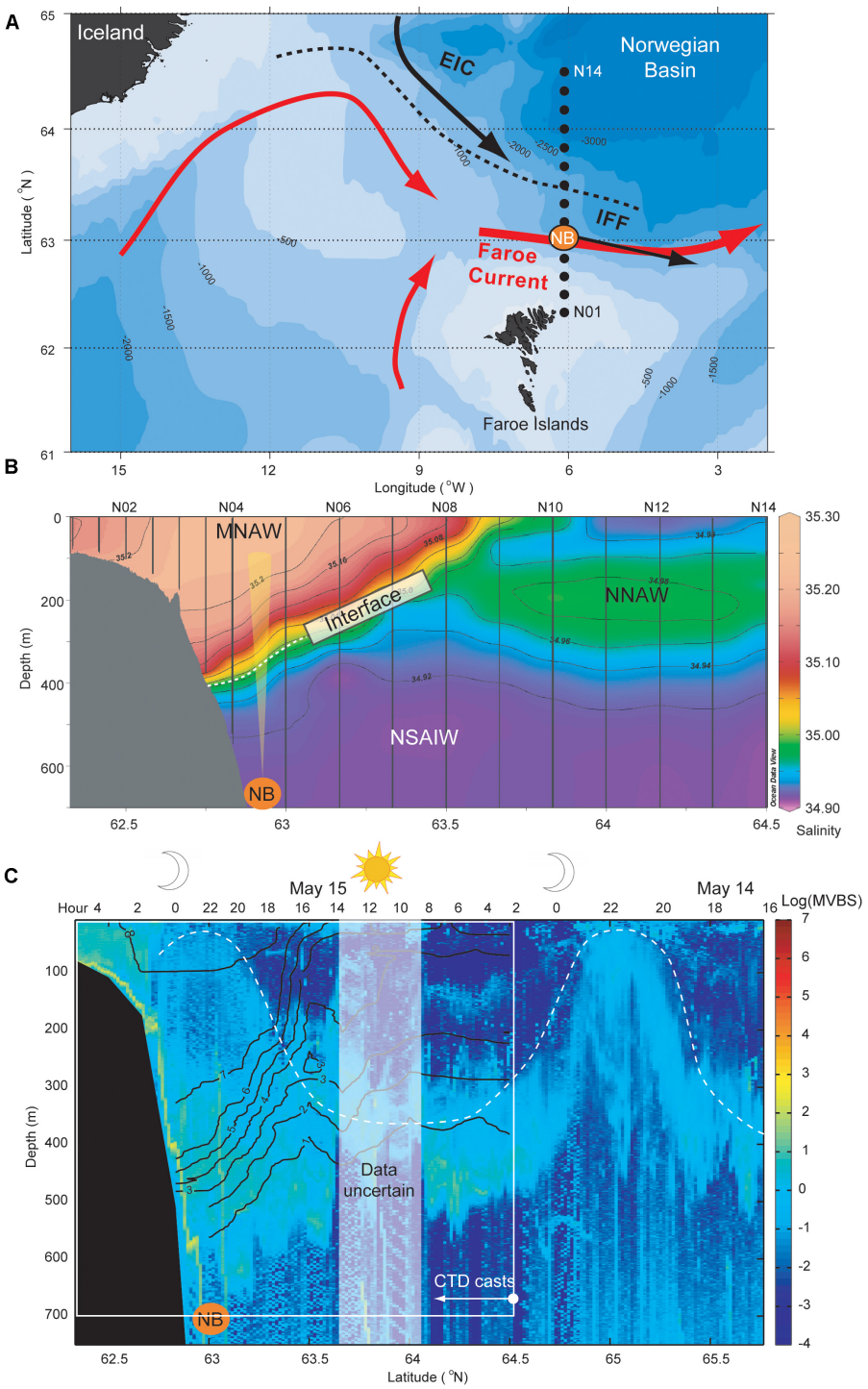

FIGURE 1 | (A) Bathymetry and circulation of the study area. Standard hydrographic stations are illustrated as black dots along Section N (06.08°W). EIC, East Icelandic Current; IFF, Iceland-Faroe Front. The position of ADCP mooring NB is here (and in the panels below) illustrated as an orange dot, and the average observed current direction is shown with the black arrow. **(B)** Average salinity along Section N based on CTD (Conductivity, Temperature, Depth) observation by R/V Magnus Heinason in the period June 2013 to May 2015, and the position of the main interface separating warm Atlantic waters from colder underlying waters is emphasized. The figure is plotted using Ocean Data View (Schlitzer, Reiner, Ocean Data View, https://odv.awi.de, 2020). **(C)** acoustic transect along an extended Section N during May 14–15, 2018. Data obtained from the ship-mounted echo-sounder on-board R/V Magnus Heinason, are here provided as the mean value backscattering strength (MVBS) over 1 m depth intervals and 10 min "distance" (the ship cruises at about 10 knots) intervals. The values are furthermore log-transformed, in order to emphasize the diffuse small biota, which are focus of the present study. The position of the 1–8°C isotherms, obtained from concurrent CTD casts are overlaid with black lines, and the diel vertically migrating layer is emphasized with a white dashed curve. Duration of day and night are illustrated at the top of the subfigure, and the white rectangle in **(C)** outlines the coverage of panel **(B)**. MNAW, Modified North Atlantic Water; NNAW, Norwegian North Atlantic Water; NSAIW, Norwegian Sea Arctic Intermediate Water.

section. In 1997, the hydrographic data set was complemented by ADCP measurements, which were deployed at depth along the section. The core data set of this study consists of ADCP measurements obtained at standard site NB, which is near the core of the Faroe Current (**Figure 1**).

CTD Data

The hydrographic database consists of conductivity-temperature-depth (CTD) stations sampled between June 2013 and May 2015 with a Sea-Bird Electronics SBE 911plus CTD. These stations were used to map the hydrographic field of the Iceland-Faroe MNAW inflow toward the Arctic (Hansen et al., 2010). On each cruise, all CTD casts extended down to 1,300 m, except for shallower stations in the southern part and the northernmost station on Section N, which extended to 2,000 m. Station spacing was equidistantly 10 nautical miles. The CTD has been mounted with a multi-bottle Sea-Bird SBE32 Carousel water sampler holding 12 5 L bottles. Conductivity data from the CTD probes were corrected after the cruise with salinity measurements of water samples using a salinometer (Guildline Autosal 8400A) referenced to IAPSO standard seawater. The calibration of the temperature sensor was accurate to < 0.001 K for all surveys. CTD readings of salinity were calibrated to an accuracy < 0.005.

ADCP Data

While the ADCP measurements were mainly used to estimate the volume transport of MNAW through the standard section (e.g., Hansen et al., 2003, 2010), we here present the first utilization of the acoustic backscatter time series measurements derived from a moored 76.8 kHz Workhorse Long-ranger ADCP (Teledyne RD Instruments, United States) to provide valuable insights into the dynamics of mesopelagic species. In the study, two consecutive deployments at a standard position between stations N04 and N05 from the period June 2013–May 2015 have been analyzed (**Table 1**). In the deployments, the instrument was moored in an upward-looking configuration at ∼700 m depth. The ADCP has four transducers which are oriented with a slant angle of 20° off the vertical axis. In order to cover the whole water column above the ADCP, it was set to have 70 bins and bin lengths of 10 m. The temporal sampling interval was set to 20 min with 10 equidistant pings per ensemble; the selected number of pings was based on the instrument battery consumption.

Ship-Mounted Echo Sounder Data

During May 14–15, 2018, a combined acoustic-hydrographic (CTD) transect was made by FAMRI's research vessel, R/V Magnus Heinason, following Section N and extending further north to 65.8°N. The acoustic data were collected from calibrated scientific echo sounders (Simrad EK60) using an operating frequency of 38 kHz. All transducers are calibrated with a standard calibration sphere (Demer et al., 2015) prior to the surveys.

Data Analysis

Computation of Mean Volume Backscattering Strength (MVBS)

The echo intensities E recorded with the ADCP were given in an automatic gain control count scale of 0–255. Following the version of the sonar equation introduced by Deines (1999) and updated by Mullison (2017), they were converted to the MVBS (dB):

$$MVBS = C + 10\log\left[(T_x + 273.16)R^2\right] - L_{DBM} - P_{DBW} + 2\alpha R + 10\log\left(10^{k_c(E-E_r)/10} - 1\right)$$

with: C = built-in system constant including transducer and noise features (dB), T_x = temperature of the transducer (°C), R = range along the beam to scatterers (m), L_{DBM} = 10log10 (transmit pulse length/meter), P_{DBW} = 10log10 (transmit power/Watt), α = coefficient of sound absorption for seawater (dB/m), k_C = beam-specific scaling factor (dB/count). The noise level (E_r) of all four beams was determined from the minimum values of RSSI (Received Signal Strength Indicator) counts obtained in the remotest depth cell, when the sea surface was outside the ADCP range. The position of the DSL was estimated as the depth at maximum daily (24 h) averaged MVBS within the depth range 170–600 m. Similar DSL night- and day- depth estimates were obtained when averaging over only the dark hours and the light hours, respectively. As a second approach, the weighted mean depth (WMD) of backscatter was used to determine the mean depth of the DSL. The WMD was calculated for each MVBS profile following the equation:

$$WMD = \sum_{i=1}^{N} Sv_i \, z_i / \sum_{i=1}^{N} Sv_i$$

with: Sv_i = volume backscattering coefficient, z_i = corresponding depths.

Estimation of the Migration Velocity

We analyzed the seasonal variation of the migration velocity by calculating average diel cycles of the vertical velocity obtained by the ADCP for consecutive months (see **Figure 7**). For improved statistical significance when analyzing vertical velocity, we averaged the diel cycles between depths of 100 and 500 m. Because the uncertainty of single-ping data from the ADCP in the velocity is too large, averaging is applied in order to reach acceptable levels. A single-ping uncertainty reading 118 mm s^{-1} is provided by the manufacturer for the instrument provided in

TABLE 1 | ADCP deployments between station N04 and N05 on Section N (see **Figure 1**).

Deployment	Latitude	Longitude	Bottom depth (m)	Instrument depth (m)	Observational period	Duration (days)
1	62.91°N	6.08°W	964	710	June 9, 2013–May 15, 2014	341
2	62.92°N	6.08°W	953	700	June 6, 2014–May 25, 2015	354

long-range mode and a bin length of 10 m. Since individual pings are independent, measurement uncertainty can be reduced by the following equation (Teledyne RD Instruments, 2018):

$$\frac{\textit{Statistical uncertainty for one ping}}{\sqrt{\textit{Number of Pings}}}$$

The sampling interval was set to 20 min with 10 pings averaged per ensemble i.e. 30 pings per hour. For weekly averages, the number of pings is therefore 7·24·30 = 5,040 and the statistical uncertainty of the velocity measurements reduces the standard errors of [118/($\sqrt{}$5,040 mm s^{-1})] = 1.7 mm s^{-1}. Vertical migration velocities are also estimated from the "slope" velocity of individual MVBS contours, using the method introduced by Luo et al. (2000) and used by Cisewski et al. (2010). The migrating layer of enhanced MVBS is fit by either a hyperbolic tangent function or a parabolic function. Vertical migration velocities were then calculated between each successive data point as the change in depth (m) per time (s). The downward migration phase of the parabolic fit is defined as the time range that runs from the starting point to the vertex of the parabola, and the upward migration phase as that from the vertex to the endpoint. In the case of the hyperbolic tangent fit, we define the starting point and the endpoint as that depth where the change in depth of two successive data points exceeds 0.5 m. **Table 2** gives an overview of the estimated velocities.

Analysis of the Vessel-Mounted Echo Sounder Data

The echo-sounder data were scrutinized using the software Echoview®. Scrutinization involves identifying and aggregating acoustic data, based on knowledge gained from previous repeated visits of the area and from aimed mid-water trawling on the acoustic targets, segregating the data into regions of identifiable fish species. The echo-sounder data were averaged into 1 m × 10 min (1–2 nautical miles, with the typical cruise speed of the vessel) bins, providing MVBS.

Interface Depth

The ADCP mooring is located near the core of the Faroe Current (**Figure 1**), and the eastward current component (*U*-component) gives a valid representation of the mean flow, which generally is directed slightly south of due east (**Figure 1A**). We estimate the vertically undulating lower boundary of the Faroe Current—the interface—as the depth where the vertical *U*-profile is most flat, i.e., locating the maximum of the gradient dU/dz, where z is depth. Daily averaged *U*-profiles are used in order to avoid the complexity of tides, and only days when the Faroe Current jet strikes the mooring (criteria: currents at 200 m > 2 × currents at 500 m) have been utilized. Data from both deployments have been used for this test, providing 515 daily profiles of the vertically shaped Faroe Current and the same number of interface depths. Direct observations of the interface depth using a Pressure Inverted Echo Sounder (PIES) (2017–2019, Hansen et al., 2019) confirms that the *U*-profile interface depth estimate closely reflects the vertical variability of the 4°C isotherm (R = 0.64) over the mooring.

TABLE 2 | Mean and maximum slope velocities, as well as range of migrating scatterers estimated from the slope velocities of the different scattering layers.

Period	Summer solstice					Autumnal equinox					Winter solstice					Spring equinox				
	Ascent velocity (mm s^{-1})		Descent velocity (mm s^{-1})		Range (m)	Ascent velocity (mm s^{-1})		Descent velocity (mm s^{-1})		Range (m)	Ascent velocity (mm s^{-1})		Descent velocity (mm s^{-1})		Range (m)	Ascent velocity (mm s^{-1})		Descent velocity (mm s^{-1})		Range (m)
	Mean	Max	Mean	Max		Mean	Max	Mean	Max		Mean	Max	Mean	Max		Mean	Max	Mean	Max	
2013–2014	−4	−8	+4	+8	70–150	−4	−8	+4	+8	70–160	−11	−21	+11	+21	70–210	−19	−36	+19	+36	70–380
						−12	−34	+12	+34	70–300						*−15*	*−46*	*+15*	*+46*	*290–600*
2014–2015	−4	−7	+4	+7	70–150	−4	−8	+4	+8	70–160	−12	−21	+11	+21	70–210	−19	−36	+19	+36	70–380
						−12	−34	+13	+34	70–300						*−15*	*−46*	*+15*	*+46*	*240–600*
Average	−4	−7	+4	+7		−8	-21	+8	+21		−11	−21	+11	+21		−16	−30	+16	+30	

DSL values in Italics.

RESULTS

Hydrography

Section N extends meridionally from the Faroe Shelf to the southern Norwegian Sea. The typical properties of this standard section are illustrated by the averaged salinity from the seven occupations of the section in the observational period June 2013 to May 2015 in **Figure 1B**. The southern part of this transect is dominated by a wedge of warm and salty MNAW extending horizontally from 62.33 to 63.25°N (station N01–N07) and vertically from an average of 400 m to the surface. Strong gradients both in salinity and temperature mark the position of the main interface between overlying MNAW and the cold and low-saline underlying subarctic water masses. The interface outcropped—average (2013–2015)—at the surface in the vicinity of standard hydrographic station N09, as the Iceland-Faroe Front. The average depth of the interface at the ADCP mooring site was about 380 m (**Figure 1B**).

A Ship-Mounted Echo Sounder Transect

A broad view of the distribution of backscatter-inducing biota north of the Faroe slope is provided by the vessel-mounted echo sounder transect along Section N and further north to 65.8°N (**Figure 1C**). The research vessel started in the north on May 14, 2018 and the lateral longitude axis (x-axis) is therefore also a time axis increasing southward, with the duration of night and daytime illustrated above the figure. In addition, CTD casts were made and isotherms have been overlaid in order to portray the position of the Faroe Current during those days. A DSL is evident throughout this transect at 300–500 m depths. The backscatter in this layer is, however, stronger and reaches deeper within the Faroe Current compared to the region farther north. On top of this, there is a diffuse scattering layer which exhibits DVM—located in the near-surface layer during night and congregating in a deep layer during daytime (dashed line in **Figure 1C**). North of the current, the DSL empties when the biota ascends toward the surface at night. Within the Faroe Current, on the other hand, elevated MVBS values were observed both within the DSL and near the surface during the night.

Long-Term and Diel Variation in the Vertical Distribution of MVBS

Mean 24-h cycles of the MVBS vertical distribution (with each cycle derived from 1 week of data) for 98 consecutive weeks (June 2013 to March 2015, **Figure 2**) reveal a variety of bands of high backscatter. The mean weighted depth (MWD), overlaid the depth-time color image, illustrates the combined variability of two dominant patterns (i) a long term (>a week) variability of both the intensity and depth of the DSL and (ii) clear DVM, whose activity varies through the year. The DVM is most pronounced during the later winter/spring months March-April, albeit also invigorated during the fall (late August and September). The DVM activity is relaxed during mid-summer (June–July) and mid-winter (November and December). During these seasons, the highest MVBS is observed at the DSL, which generally is located at the mean depth of the interface at the ADCP mooring site (horizontal line at 380 m in **Figure 2**), although the DSL was elevated above this depth during summer 2014 (**Figure 2B**). No statement can be made about the dynamics in the top few tens of meters, because of the limited reach of the ADCP data. We will hereafter first address the slowly varying DSL, and then discuss the seasonally varying DVM.

A Close Link Between the DSL and the Interface

The fact that the daytime residence layer—the DSL was located at 400–500 m depths, both within the Faroe Current and far north of it during the 2 days of the ship-mounted echo sounder transect (**Figure 1C**, 14–15 May, 2018) could indicate a broad light-regulation of the vertical position of the DSL. On the other hand, the intensified backscatter at the base of the Faroe Current, whose closely aligned isotherms during these days intersected the Faroe slope at 450–500 m depths (**Figure 1C**), could indicate an additional link to the physics of this current. The DSL position at the ADCP mooring is clearly associated with the interface under the Faroe Current (see section "Interface Depth" and **Figure 3**). This link is very close during the latter half of the year (June–January, R = 0.82), but less direct during the late winter/early spring months, February to April (R = 0.66). The interface was elevated far above its mean depth during July 2014, which can explain the above mentioned shallow DSL position during this month (**Figure 2B**).

The 515 current profiles from the ADCP deployments were first aligned to the vertically undulating interface reference frame (centered at the steepest dU/dz gradient). Then all the profiles were averaged, in order to illustrate the mean vertical structure of this flow, relative to the interface depth (**Figure 4**). This shows that the eastward flow increases from ∼50 mm s^{-1} 20 m below the interface to ∼130 mm s^{-1} 20 m above the interface. The MVBS profiles were similarly aligned to the interface reference frame and averaged, which reveals that the DSL (MVBS peak) is typically located around 10–30 m below the interface depth under the Faroe Current (**Figure 4**).

Diel Vertical Migration

In addition to stochastic motion, short term variability in ocean currents around the Faroe Islands are primarily influenced by the semi-diurnal tidal constituents M_2 (12.42 h, 1.93 cpd), S_2 (12 h, 2.00 cpd), and N_2 (12.66 h, 1.90 cpd) and secondarily by the diurnal constituents O_1 (25.82 h, 0.93 cpd) and K_1 (23.93 h, 1.00 cpd) (e.g., Larsen et al., 2008). Distinct elevations of energy neighboring the semi-diurnal tides M_2 and S_2 are visible in the power spectra of the horizontal current speed at the ADCP mooring, followed by a secondary peak at the diurnal tidal frequencies (O_1 and K_1, **Figure 5A**). In contrast, a diel peak dominates the power spectrum of the vertical velocity (w), while the semidiurnal constituents represent less energy (**Figure 5B**). The enhanced diel energy of w is likely linked to the day-night cycle.

Complex interplay between the slowly undulating DSL/interface and the rapid, although seasonally varying, DVM during the years summer 2013–summer 2015 (**Figure 2**), is

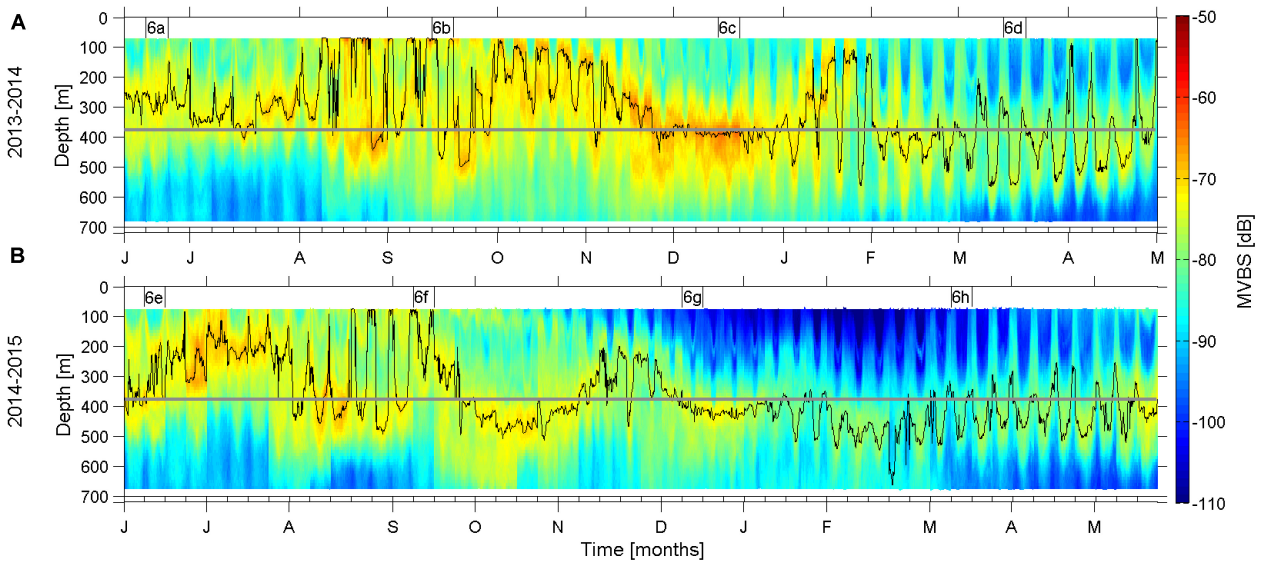

FIGURE 2 | Annual time series of weekly averaged 24 h cycles of mean volume backscatter strength from June 2013 to May 2014 **(A)** and from June 2014 to May 2015 **(B)**, i.e., each weekly slot shows the average 24 h cycle of that week. Overlaid is the weighted mean depths (WMD) (black lines). The **Figures 6A–H** at the top of the panels refer to the weeks, illustrated in the corresponding **Figure 6** panels. The average depth of the interface (∼380 m, see **Figure 1B**) is illustrated with a horizontal gray line.

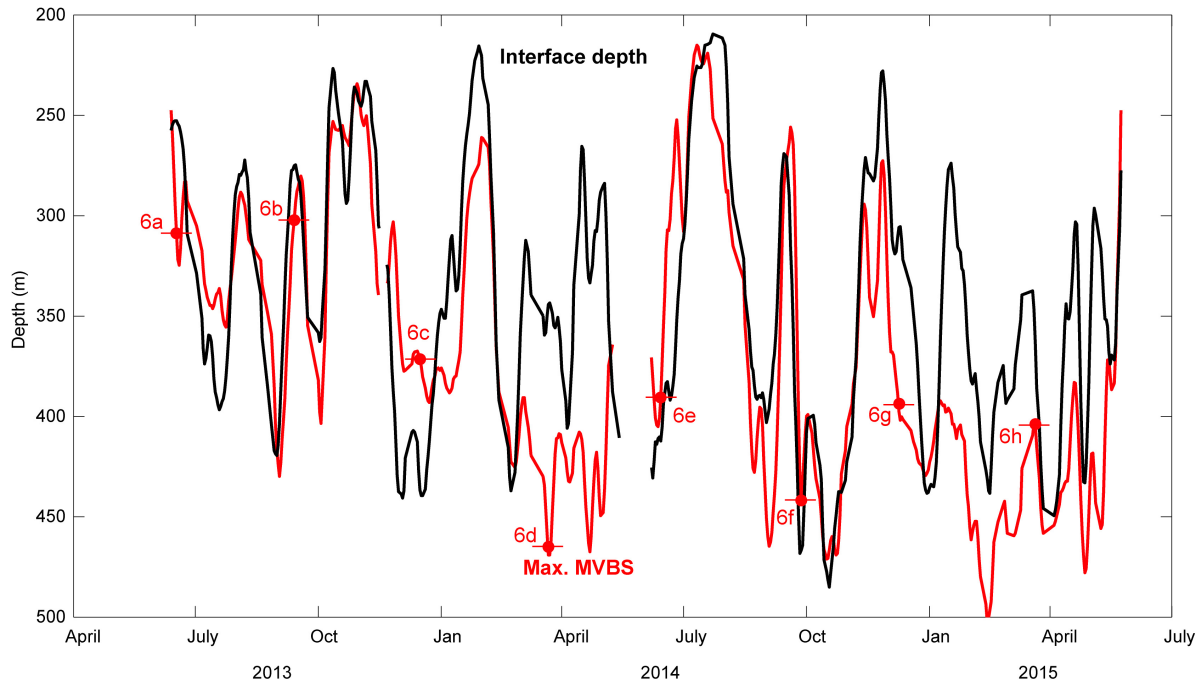

FIGURE 3 | Temporal variability of the depth of the *interface* (black) and the strongest mean volume backscattering strength MVBS (red) based on the ADCP deployments near the core of the Faroe Current jet. A 5 days low-pass filter has been applied to the daily averaged data. The red strikethrough dots and the associated labels refer to the days, illustrated in the corresponding panels in **Figure 6**.

here discussed for the four distinct seasons: Summer solstice (20–21 June), autumnal equinox (22–23 September), winter solstice (20–22 December) and spring equinox (20 March). Weekly mean diel MVBS patterns over these seasons are discussed, in relation to the sun angle calculated using the solar position algorithm by Reda and Andreas (2004) (shown in the top panels in **Figure 6**), and the directly observed vertical velocity, w (lower panels in **Figure 6**). The approximate depth of the DVM layers are

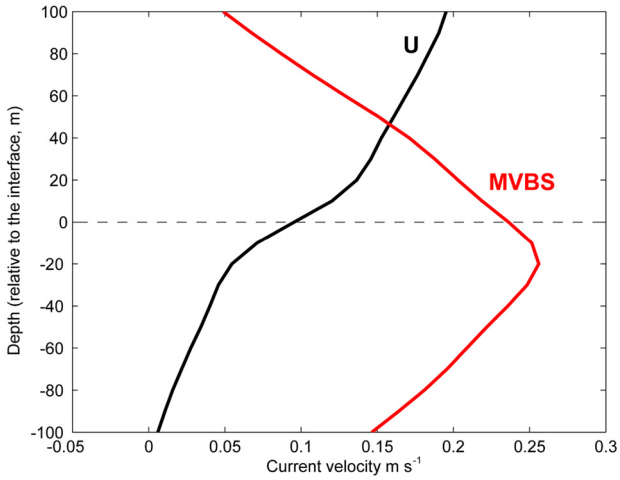

FIGURE 4 | Currents and backscatter at the ADCP mooring near the core of the Faroe Current jet. The averaged (2013–2015) zonal current velocity profiles (*U*-component, black) and the normalized mean volume backscattering strength MVBS (red, not to scale), both vertically centered at the vertically shifting interface under the Faroe Current (**Figure 3**).

emphasized with dashed curves, and identical curves drawn for both years, which illustrates the recurrence of the here discussed dynamics. Gray horizontal lines in each subpanel in **Figure 6** represent an approximate position of the interface during the 8 weeks, highlighted in **Figure 3**.

Summer Solstice (Sunrise: 02:18, Sunset: 22:34, UTC)

A broad band of strong MVBS is observed in the 300–500 m depth interval—with a tendency of congregation at the interface (**Figures 6A,E**). Low MVBS values are observed below 500 m. A DVM layer descends from the near-surface photic zone (<70 m) just before sunrise, reaches approximately 200 m depth around noon, re-ascends and reaches the near-surface zone shortly after sunset. The DVM layer does not reach the interface, which during both years was located at between 300 and 400 m. By fitting a mathematical function to this scattering layer (see section "Estimation of the Migration Velocity") the mean and maximum up- and downward migration velocities are ± 4 and ± 8 mm s^{-1} in 2013 and ± 4 and ± 7 mm s^{-1} in 2014, respectively (**Table 2**). The curve-fitted vertical velocities during the other seasons are also provided in **Table 2**, and will not be reiterated in the subsequent text. Since between 40 and 75% of all measured vertical ADCP velocities within the top 150 m are invalid around the summer solstice 2013 (**Figure 6A**), those data were excluded from our analysis. During 2014, a band of negative values is evident below the visibly descending DVM layer (0–6 a.m., 200–300 m depths, **Figure 6E**), while a band of positive values of *w* aligns with the ascending DVM layer after noon.

Autumnal Equinox (Sunrise:06:05, Sunset:18.28, UTC)

Generally, there is increased MVBS at the interface and elevated backscatter observed below 600 m depth (**Figures 6B,F**). Very high MVBS occurred near the surface during the dark hours, and the associated biota descended around sunrise in two distinct layers—a slowly migrating layer to 100–150 m depths and a faster layer reaching 300 m depth during noon (see **Table 2**). This deeper DVM seems to have reached, and potentially crossed, the interface during 2013 (**Figure 6B**), while it only approached the interface during 2014 (**Figure 6F**). During 2014, both the descending and ascending motion of the deeper DVM layer was clearly captured by the vertical velocity data (**Figure 6F**). Negative values of *w* also coincided with the descending scattering layer during 2013 (**Figure 6B**), while positive *w* values were located slightly below the rising layer this year.

Winter Solstice (Sunrise:10:00, Sunset: 14:45, UTC)

A marked and stationary DSL was associated with the interface, which was located at nearly 400 m depth during both years (**Figures 6C,G**), and high MVBS values were observed below 500 m. DVM is evident in the upper 200 m, where waters are cleared for backscatterers during the few sunlit hours. A slight depression is identifiable in the near-interface DSL during the lit hours, although the associated motion is too weak for an estimation of vertical migration velocities using the curve fitting method (section "Estimation of the Migration Velocity"). The vertical velocity data (*w*) do not reveal any discernible patterns during this season.

Spring Equinox (Sunrise:6:19, Sunset: 18:45, UTC)

This is the season with strongest DVM, and the interface is only vaguely associated with elevated values of MVBS (**Figures 6D,H**). Two distinct DVM layers are evident—one migrating from the near-surface to about 380 m, and a deeper layer that approaches 600 m depth during noon. The shallower layer approaches the interface, while the deeper migrators approach a deep DSL during noon which, especially in 2014 (**Figure 6D**), also was occupied by biota during the night. During the dark hours, at least a portion of the biota constituting the deep migrators resides in a diffuse 150–400 m depth layer, and it remains uncertain whether or not these species actually reached the near-surface waters during the night. Migration timing of the layers is synchronized, descending at sunrise and ascending during sunset, and the vertical motion is sharply expressed by *w*. The highest values of *w* are observed at 100–300 m depths—when both layers are in close proximity—while the continued descent of the deeper layer is associated with lower *w*. The fastest migration velocity of 46 mm s^{-1} obtained by curve-fitting method (**Table 2**) is assigned to the deep migrators.

Seasonal Variation of the Vertical Velocity

To examine the seasonal variability of the migration velocity, we calculated mean diel cycles of *w* (averaged between 100 and 500 m depth) for consecutive months (**Figure 7**) following the method used by Cisewski et al. (2010) (see section "Estimation of the Migration Velocity"). This analysis includes the times of local sunrise and sunset at the mooring position (dashed curves in **Figure 7**) in order to analyze the role of the day-night light cycle.

The temporal distribution of ascent and descent velocities peak symmetrically around noon, which reveals a clear dependence on the sun angle. As the day length shortens

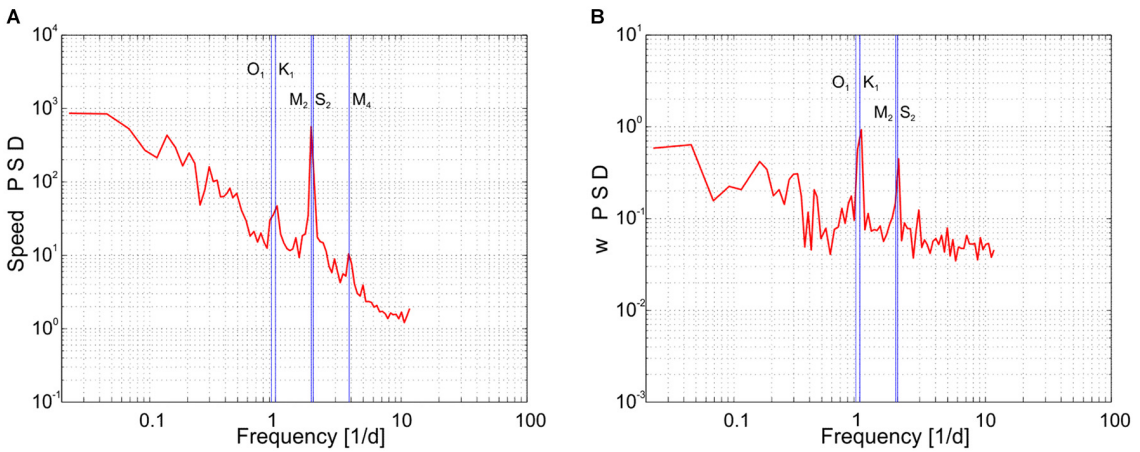

FIGURE 5 | Power Spectral Densities computed using horizontal current speeds **(A)** and vertical velocities **(B)** obtained by the moored ADCP averaged vertically between 100 and 200 m. Labels were given to single peaks at tidal constituent frequencies (O1, K1, M2, S2, and M4).

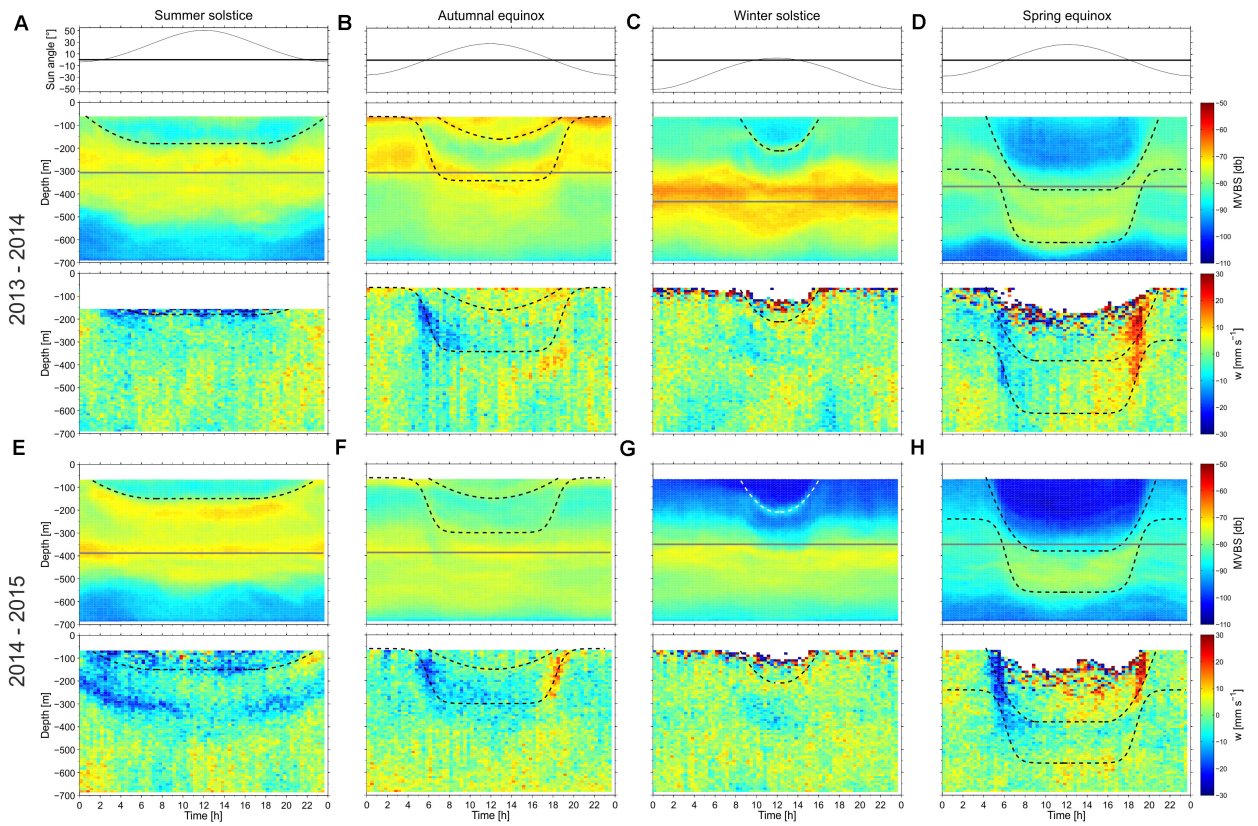

FIGURE 6 | Mean diel cycle of the sun angle (upper panels), mean volume backscattering strength MVBS (mid-panels) and Doppler vertical velocity *w* (lower panels) estimated for four different weeks near **(A,E)** summer solstice, **(B,F)** autumnal equinox, **(C,G)** winter solstice and **(D,H)** spring equinox of the years 2013–2015. The average interface depth over each individual week (see **Figure 3**) is illustrated with a horizontal gray line, and the discussed backscatter layers are emphasized with dashed curves.

between July and winter solstice, the downward and upward migration peaks shifted by around ± 1 h per month. The scatterers start to descend about 1–2 h before sunrise, and highest downward velocities are observed prior to sunrise (red band in **Figure 7**). Similarly, the highest upward velocities are observed after sunset, and the ascent ceases about 1–2 h after sunset (green band). Negative values of *w*, related to downward migration, are evident throughout the year, with

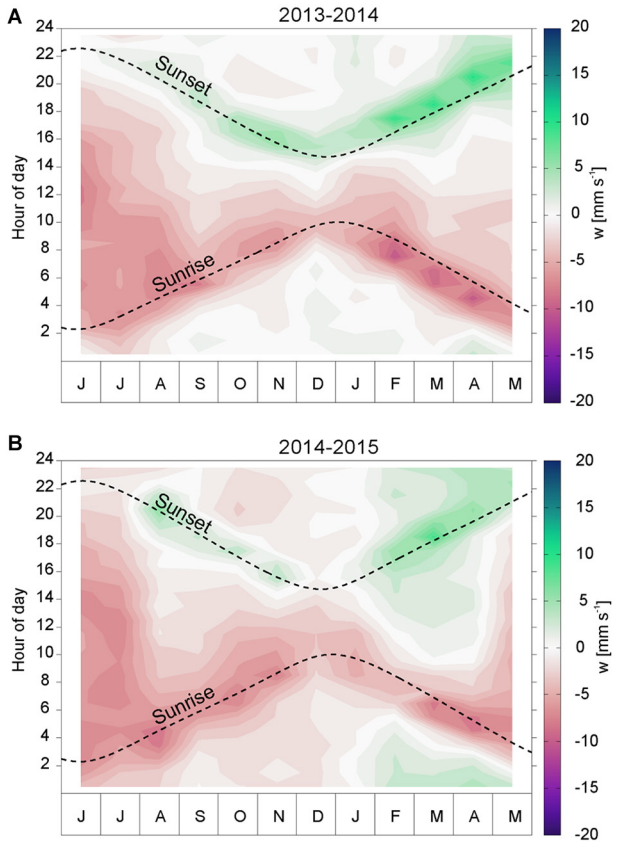

FIGURE 7 | Seasonal variation of the diel vertical migration velocity averaged between 100 and 500 m depth from June 2013 to May 2014 **(A)** and from June 2014 to May 2015 **(B)**. Contour intervals are 1 mm s-1. Dashed lines show the times of local sunrise and sunset.

an indication of higher values during late winter months (February to April). During the summer months (June and July) downward velocities are observed in the upper 200 m of the water column through most of the 24 h cycle. The ascent velocities are highest during the late winter and spring months (December–May, green) and barely visible during late summer and fall.

Depth-Averaged MVBS and Characteristics of the Faroe Current

Daily means of MVBS, averaged between 70 and 600 m water depth, were calculated in order to investigate the seasonality of mesopelagic biomass. The vertically averaged MVBS time series, (**Figure 8A**) reveals a clear seasonal cycle with maximum during late summer (August-September), and a minimum around the late winter/spring months (February–April). MVBS declined by about 10 dB from November 2013 to February 2014, while the larger decline over the subsequent winter amounted to nearer 15 dB. This seasonal variability of the MVBS co-varies with the monthly mean transport-averaged temperature of the eastward flowing MNAW in the Faroe Current (**Figure 8C**), estimated by a new method introduced by Hansen et al. (2020). The lowest backscatter and temperature values are observed during spring (6.34°C, **Figure 8C**) and the highest values around August-September (8.5°C). During the sampling period, the MNAW transport across Section N was relatively persistent, with an average of 3.8 Sv (**Figure 8B**), and no clear relation was found between the MVBS (**Figure 8A**) and the variability of this transports (**Figure 8B**).

DISCUSSION

The presented MVBS data have revealed three dominant variability patterns: (i) a seasonal cycle of the depth-averaged backscatter (70–600 m), with a maximum during the late summer and a minimum during late winter/spring, (ii) a marked DSL exhibiting relatively slow vertical undulations (>1 month time scale) within the 250–450 m depth range, and (iii) DVM, which are active during spring and fall, and more quiescent during mid-summer and mid-winter. These signals must somehow be related to lateral transports of MNAW over the main interface, lateral transports of subarctic water masses under the interface, and/or vertical migration-motivating cues.

Physical Drivers of the Main Signals

No link is found between the depth-integrated MVBS and the transport of MNAW, while the MVBS maximum during spring concurs with minimum in transport-averaged temperature of the MNAW, and minimum in backscatter during fall concurs with the highest temperatures. The presented records are, however, too short for making any firm conclusions on long-term co-variability.

The variable depth of the DSL is linked to vertical undulations of the interface, with the highest backscatter located immediately below the interface. This DSL-interface link is likely due to the accumulation of biomass (backscatters) along the interface, more so than a physical reflection from the sea water density gradient across it. It is very close during summer and fall and less direct during late winter and spring, when the DVM activity is strongest (see below). By associating the DSL-interface link with a recently discovered coupling between the interface depth and the circulation strength of the Norwegian Sea Gyre (NSG) (Hátún et al., In Prep), we are able to view this MVBS pattern in a larger oceanographic context. A strong (weak) NSG, induced by cyclonic anomaly of the wind stress curl of the Norwegian Sea, is associated with a shallow (deep) interface and thus also a shallow (deep) DSL. Also, a recently discovered Iceland-Faroe Slope Jet (IFSJ), running at depth under the Faroe Current, is seen to impact the Faroe Current interface (Semper et al., 2020). Thus an intensified IFSJ elevates deep (dense) isopycnals in the vicinity of the ADCP mooring (Semper et al., 2020), but the influence of this deep flow on the relatively shallow interface has not yet been discussed. We are not aware of any previous study which links acoustic backscatter signals to major oceanographic features. It should, for completeness, be mentioned that short-term fluctuations of the interface depth (**Figure 3**) are also associated with passing weather systems, tides and meso-scale variability

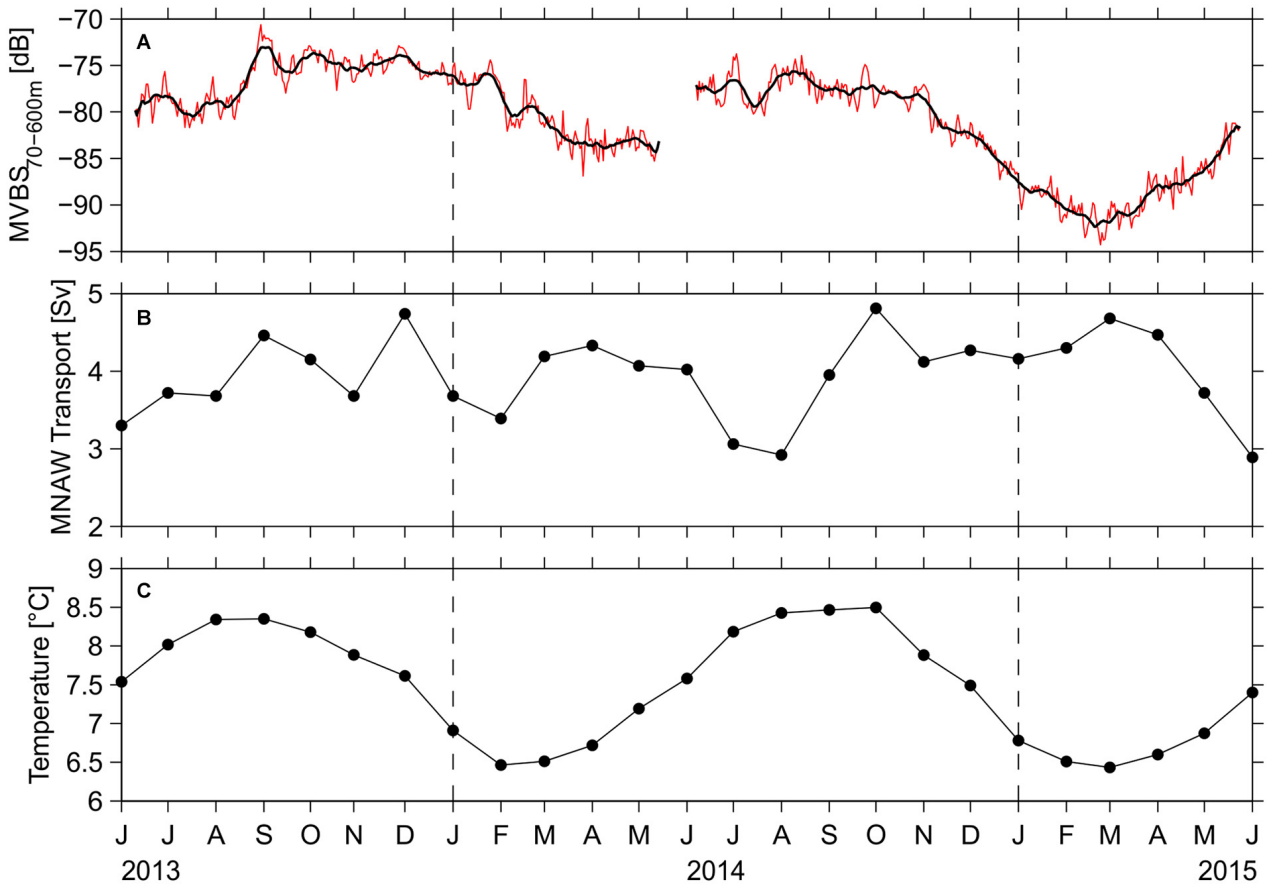

FIGURE 8 | Seasonal variability in mean volume backscattering strength and related environmental parameters: **(A)** depth-averaged (70–600 m) mean volume backscattering strength (daily averages as red line and 7 days running mean as black line), **(B)** monthly averaged transports of Modified North Atlantic Water (MNAW) in the Faroe Current, **(C)** monthly transport-averaged temperature of the MNAW (Hansen et al., 2020).

along the Iceland-Faroe Front (Hansen and Meincke, 1979) and a thorough investigation of the controlling mechanisms will be complex.

DVM is a behavioral response to a combination of exogenous factors (e.g., light, temperature, salinity, and oxygen) and endogenous factors (e.g., sex, age, state of feeding, and changes in behavior and physiology) (Forward, 1988). Based on MVBS and *w* data from the ADCP, we have demonstrated that normal DVM—closely related to the astronomical daylight cycles—is a persistent behavioral pattern throughout the year. Our results thus support the hypothesis for light as the most important exogenous cue for the timing of DVM within the Faroe Current, and likely also for the southern Norwegian Sea as a whole. This is in agreement with studies from several disparate regions (Roe, 1974; Forward, 1988; Haney, 1988; Ringelberg, 1995), and as an example did Staby et al. (2011) show a similar relationship between the seasonally changing daylight cycle and the timing of the DVM for Müllers pearlside in Masfjorden Norway. There, biota also start to migrate downwards shortly before sunrise and attain again the surface shortly after sunset (Staby et al., 2011). We can, however, not answer the question whether the absolute intensity of light or the rate of change of light were used as an exogenous stimulus for DVM by the migrators because of a lack of further information on the light field within the water.

During summer and winter solstices, we only observe relatively shallow migration, which is unlikely to interfere with the interface (**Figures 6A,E,C,G**). However, the deeper migration during autumnal equinox does reach depth levels of the interface (**Figures 6B,F**), and the involved species could be motivated by this sharp water mass boundary. During spring equinox, the shallower DVM layer reaches the interface, while the deeper DVM layer descends far below the interface (**Figures 6D,H**), and the migrators could therefore contribute to active vertical carbon transport in this area. Thus, our results might be useful for a regional parameterization of the DVM in biogeochemical models.

In summary, the seasonal changes in DVM activity and the depths of different migration layers cannot be explained by light intensity alone, and a better understanding likely requires a consideration of both the physical environment and the species constituting the backscatter layers (section "Reflections on Species Involved in Various Patterns").

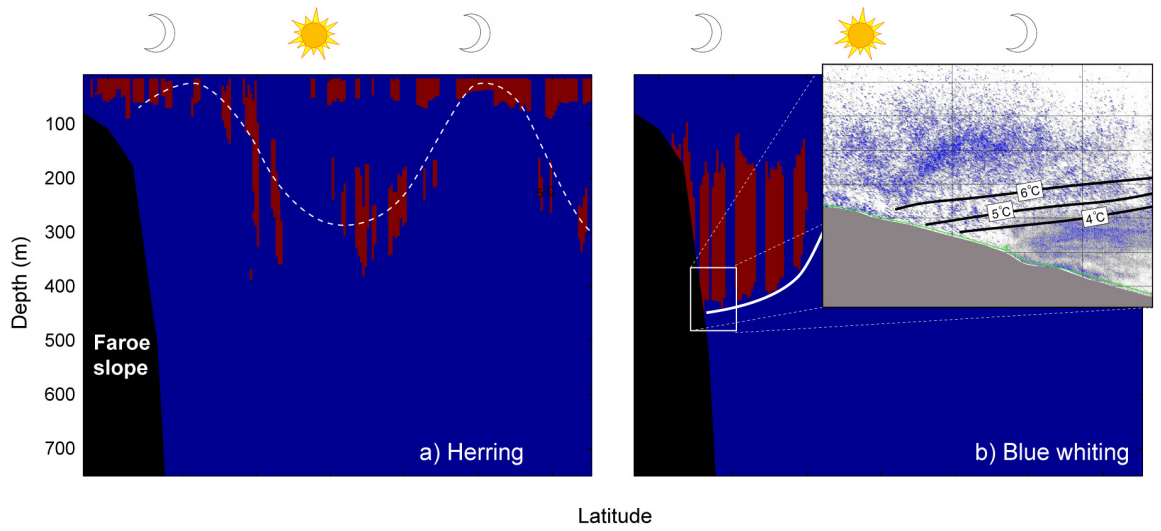

FIGURE 9 | Scruitinized acoustic backscatter from the ship-mounted echo-sounder. Distribution of **(A)** herring and **(B)** blue whiting. Times of day and night are cartooned with a sun and a moon, respectively. The dashed undulating curve in **(A)** illustrates DVM in the herring distribution and the white line in **(B)** illustrates the position of the interface (see **Figure 1C**). The inset panel in **(B)** shows acoustic backscatter, in the location where the interface intersects the seafloor (see **Figure 1C**). This is obtained as a screen shot from the software Echoview®, and the position of the three isotherms is estimated from **Figure 1C**.

Migration Velocities

Our results have shown that the migration velocities and daily residence depths vary from season to season (see **Table 2**). The slopes of the scattering layer, which reached about 200 m depth during noon, revealed vertical migration with average speeds of ± 10–20 mm s^{-1} and maximum speeds of ± 34 mm s^{-1}. The layers reaching down to 600 m exhibited similar average speeds while maximum speeds reached ± 46 mm s^{-1}. This is roughly in accordance Bianchi and Mislan (2016) who, based on a large number of cruises with ship-borne ADCPs in the subarctic regions of the North Atlantic, reported vertical migration velocities of 40–50 mm s^{-1}.

The directly observed vertical migration velocities in **Figure 7** appear lower than the velocities estimated from the slopes (**Table 2**). This could be due both to vertical and temporal averaging of *w*, (prior to making the figure), and/or the fact that *w* also represents a background of non-migrating scatterers, which will introduce a bias into migration rate estimates yielding systematically smaller velocities (Plueddemann and Pinkel, 1989; Heywood, 1996; Luo et al., 2000; Cisewski and Strass, 2016).

Reflections on Species Involved in Various Patterns

Addressing the ecological significance of our study requires knowledge on possible species involved in the MVBS signals. Identifying species is, as mentioned, a limitation in acoustics-only studies, and the following discussion is therefore of more generalized character.

The copepods *C. finmarchicus* and *C. hyperboreus* are key species in the pelagic system in the southwestern Norwegian Sea, coupling primary production and zooplanktivorous fish (Dalpadado et al., 2000; Hirche et al., 2001). In addition to *C. finmarchicus* within the southern Norwegian Sea, continuous advection of the larger arctic *C. hyperboreus* into the study region with subarctic waters from the Iceland Sea makes this area an important feeding area for pelagic fish during their oceanic feeding phase (ICES, 2020). During late winter to spring, the overwintering copepod generation ascends to the surface layer (upper ∼50 m) (Kristiansen et al., submitted; Gislason, 2018) and are therefore out of reach for the ADCP, where they feed on the initiated spring bloom and reproduce (e.g., Stenevik et al., 2007; Kristiansen et al., submitted). These prey items are too small to give a direct acoustic signal (e.g., Melle et al., 1993), which was also supported by a comparison between presented MVBS data and depth-stratified zooplankton data along Section N (see **Supplementary Figure S1**).

However, we suggest that the increased near-surface zooplankton prey biomass could provide a motivation cue for vertical migration of larger biota, which, in turn, could explain the increased DVM activity during spring (**Figures 2**, **6**). The westward feeding migration of Norwegian spring-spawning herring during April-May is guided by the concentration of these copepods (Dalpadado et al., 2000; Broms et al., 2012), and expert scrutiny of the vessel-mounted echo sounder data presented in **Figure 1C** (May 14–15, 2018) shows that herring represented a part of the observed backscatter—both in the near-surface (0–50 m) zone and in the layer performing DVM between the surface and 200–300 m depths (**Figure 9A**). DVM behavior by herring is previously reported by e.g. Huse et al. (2012). Backscatter observed within the uppermost 200 m of the Norwegian Sea is, in addition to herring, likely composed of Müllers pearlside and krill (euphausiids); and like herring, Müllers pearlside migrate very close to the surface (closer than the minimum detection range of the echo sounder) during night, and down into an

intermediate layer at 200–300 m depth during the day (Melle et al., 1993; Torgersen et al., 1997; Knutsen and Serigstad, 2001; Staby et al., 2011).

Blue whiting also enters the study region during May (ICES, 2020), where they typically occupy MNAW (Monstad, 2004) and perform some DVM within 250 m to 400 m depth levels (Stensholt et al., 2002; Huse et al., 2012). This general distribution is also evident in the scrutinized echo sounder section (**Figure 9B**), and even more sharply in the raw acoustic backscatter data at the location where the main pycnocline intersects the seafloor (**Figure 9B**, inset image). In this image, congregations of blue whiting hover over the interface, while a more fine-grained backscatter cloud is evident below the 4°C thermocline (**Figure 9B**). This cloud is reminiscent of a DSL, which typically is observed between 400 m and 500 m throughout the eastern part of the Nordic Seas, consisting of euphausiids, shrimps, jellyfish and the mesopelagic fish (Melle et al., 1993; Salvanes, 2004; Lamhauge et al., 2008). Similar predator-prey layering is observed in other locations in the Norwegian Sea and in the Greenland Sea, with planktivorous mesopelagic fish occupying the relatively warm Atlantic water and *Calanus* spp. avoiding the threat of predation by occupying the Arctic intermediate water beneath (Dale et al., 1999). These observations are in support of the predator evasion hypothesis, as the smaller animals might be "hiding" in the colder waters from the predation pressure exerted by the blue whiting.

The seasonal MVBS pattern that revealed stronger signals during the summer/autumn and weaker signals during the late winter periods (**Figures 2**, **8**), could be caused by the migratory pelagic species herring and blue whiting that congregate and feed along the productive fronts north of the Faroes from May to December (Utne et al., 2012; Trenkel et al., 2014; Strand et al., 2020). Although mackerel also is found in the near-surface layer (<50 m) in the area in the summer (ICES, 2020), it would not make any significant contribution to the seasonal variations in MVBS due to its shallow distribution and weak backscatter (Foote, 1980). Smaller mesopelagic fish found in the area such as lanternfish are expected to perform less extensive horizontal annual migrations than the three mentioned larger species (Salvanes and Kristoffersen, 2001).

CONCLUSION

New and rare insight into the diel to seasonal migration behavior of different pelagic and mesopelagic species in the southern Norwegian Sea is provided from time series of mean volume backscattering strength (MVBS) and vertical velocity from moored Acoustic Doppler Current Profilers (ADCPs) deployed along Section N crossing the Faroe Current north of the Faroe Islands. A persistent deep scattering layer (DSL) resides immediately under the Atlantic waters carried by this current, and characteristic inter-monthly variability in the DSL depth is closely correlated to the depth of the interface between warm Atlantic waters and colder subarctic waters below. We also reveal marked DVM, with timing closely associated with the day-night light cycle—descent from the photic zone 1–2 h before sunrise, and reappearance in the near-surface about 1–2 h after sunset. Vertical migration velocities and amplitudes are highest during spring, when the migration consists of two distinct layers—a shallower layer reaching the interface level (∼400 m) and a deep layer which descends to 600 m. The DVM activity is also high during fall, with a deeper layer reaching 300–400 m depths and a shallower layer descending to ∼150 m. During mid-summer and mid-winter, a single layer is observed to migrate down to ∼200 m at noon. This novel knowledge on the mesopelagic complex in the study region could potentially guide sampling of the animal species inducing the marked acoustic signals.

DATA AVAILABILITY STATEMENT

The raw data supporting the conclusions of this article will be made available by the authors, without undue reservation.

AUTHOR CONTRIBUTIONS

BC and HH coordinated the production of the manuscript. BC, HH, IK, and KL wrote the overall text. BH, SE, and JJ contributed significantly to the discussion section. All authors contributed to the article and approved the submitted version.

FUNDING

Funding for the ADCP measurements was received from the European Union 7th Framework Programme (FP7 2007–2013), under grant agreement no. 308299 (NACLIM). HH and KL were partly funded by the European Union's Horizon 2020 Research and Innovation Programme under grant agreement No. 727852 (Blue-Action).

ACKNOWLEDGMENTS

We wish to thank captains and crew on the R/V Magnus Heinason for measurements at sea and we would also like to thank two reviewers for their comments that improved the manuscript.

SUPPLEMENTARY MATERIAL

The Supplementary Material for this article can be found online at: https://www.frontiersin.org/articles/10.3389/fmars.2020.542386/full#supplementary-material

Supplementary Figure 1 | Vertical distribution of zooplankton abundance at stations **(A,B)** N04 and **(C,D)** N05 and the concurrently measured ADCP backscatter at NB at Section N (red diamonds indicate the sampling times of the Multinet). At station N05, the deepest sampling depth covered 500–1,000 m, however, here the depth is displayed down to 700 m to match the depth of the ADCP backscatter (left panels).

REFERENCES

Bianchi, D., and Mislan, K. A. S. (2016). Global patterns of diel vertical migration times and velocities from acoustic data. *Limnol. Oceanogr.* 61, 353–364. doi: 10.1002/lno.10219

Bianchi, D., Stock, C., Galbraith, E. D., and Sarmiento, J. L. (2013). Diel vertical migration: ecological controls and impacts on the biological pump in a one-dimensional model. *Glob. Biogeochem. Cycles* 27, 478–491. doi: 10.1002/gbc.20031

Broms, C., Melle, W., and Horne, J. K. (2012). Navigation mechanisms of herring during feeding migration: the role of ecological gradients on an oceanic scale. *Mar. Biol. Res.* 8, 461–474. doi: 10.1080/17451000.2011.640689

Broms, C., Melle, W., and Kaartvedt, S. (2009). Oceanic distribution and life cycle of *Calanus* species in the Norwegian Sea and adjacent waters. *Deep Sea Res. II Top. Stud. Oceanogr.* 56, 1910–1921. doi: 10.1016/j.dsr2.2008.11.005

Burd, B. J., and Thomson, R. E. (2012). Estimating zooplankton biomass distribution in the water column near the Endeavour Segment of Juan de Fuca Ridge using acoustic backscatter and concurrently towed nets. *Oceanography* 25, 269–276. doi: 10.5670/oceanog.2012.25

Cisewski, B., and Strass, V. H. (2016). Acoustic insights into the zooplankton dynamics of the eastern Weddell Sea. *Prog. Oceanogr.* 144, 42–92. doi: 10.1016/j.pocean.2016.03.005

Cisewski, B., Strass, V. H., Rhein, M., and Krägefsky, S. (2010). Seasonal variation of diel vertical migration of zooplankton from ADCP backscatter time series data in the Lazarev Sea, Antarctica. *Deep Sea Res. I Oceanogr. Res. Pap.* 57, 78–94. doi: 10.1016/j.dsr.2009.10.005

Cohen, J. H., and Forward, R. B. (2009). Zooplankton diel vertical migration – A review of proximate control. *Oceanogr. Mar. Biol. Annu. Rev.* 47, 77–110. doi: 10.1201/9781420094220.ch2

Dale, T., and Kaartvedt, S. (2000). Diel patterns in stage-specific vertical migration of Calanus finmarchicus in habitats with midnight sun. *ICES J. Mar. Sci.* 57, 1800–1818.

Dale, T., Bagøien, E., Melle, W., and Kaartvedt, S. (1999). Can predator avoidance explain varying overwintering depth of *Calanus* in different oceanic water masses? *Mar. Ecol. Prog. Ser.* 179, 113–121. doi: 10.3354/meps179113

Dalpadado, J., Ellertsen, B., Melle, W., and Dommasnes, A. (2000). Food and feeding conditions of Norwegian spring-spawning herring (Clupea harengus) through its feeding migrations. *ICES J. Mar. Sci.* 57, 843–857. doi: 10.1006/jmsc.2000.0573

Deines, K. L. (1999). "Backscatter estimation using broadband acoustic Doppler current profilers," in *Proceedings of the IEEE Sixth Working Conference on Current Measurement (Cat. No.99CH36331)*, San Diego, CA, 249–253. doi: 10.1109/CCM.1999.755249

Demer, D. A., Berger, L., Bernasconi, M., Bethke, E., Boswell, K., Chu, D., et al. (2015). *Calibration of acoustic instruments. ICES Cooperative Research Report No. 326*. (Copenhagen: International Council for the Exploration of the Sea), 133. doi: 10.17895/ices.pub.5494

Dypvik, E., Klevjer, T. A., and Kaartvedt, S. (2012). Inverse vertical migration and feeding in glacier lanternfish (*Benthosema glaciale*). *Mar. Biol.* 159, 443–453. doi: 10.1007/s00227-011-1822-4

Foote, K. G. (1980). Importance of the swimbladder in acoustic scattering by fish: a comparison of gadoid and mackerel target strengths. *J. Acoust. Soc. Am.* 67, 2084–2089. doi: 10.1121/1.384452

Forward, R. B. (1988). Diel vertical migration: zooplankton photobiology and behaviour. *Oceanogr. Mar. Biol. Annu. Rev.* 26, 361–393.

Gislason, A. (2018). Life cycles and seasonal vertical distributions of copepods in the Iceland Sea. *Polar Biol.* 41, 2575–2589. doi: 10.1007/s00300-018-2392-4

Haney, J. F. (1988). Diel patterns of zooplankton behaviour. *Bull. Mar. Sci.* 43, 583–603.

Hansen, B., Hátún, H., Kristiansen, R., Olsen, S. M., and Østerhus, S. (2010). Stability and forcing of the Iceland-Faroe inflow of water, heat and salt to the Arctic. *Ocean Sci.* 6, 1013–1016. doi: 10.5194/os-6-1013-2010

Hansen, B., Larsen, K. M. H., Hátún, H., Jochumsen, K., and Østerhus, S. (2019). *Monitoring the hydrographic structure of the Faroe Current. Havstovan Nr. 19-02 Technical Report*. Available online at: http://www.hav.fo/PDF/Ritgerdir/2019/TechRep1902.pdf (accessed December 15, 2020).

Hansen, B., Larsen, K. M. H., Hátún, H., and Østerhus, S. (2020). *Atlantic Water Extent on the Faroe Current Monitoring Section. Havstovan Nr. 20-03 Technical Report*. Available online at: http://www.hav.fo/PDF/Ritgerdir/2020/TechRep2003.pdf (accessed December 15, 2020).

Hansen, B., and Meincke, J. (1979). Eddies and meanders in the Iceland-Faroe Ridge area. *Deep Sea Res. A Oceanogr. Res. Pap.* 26, 1067–1080. doi: 10.1016/0198-0149(79)90048-7

Hansen, B., Østerhus, S., Hátún, H., Kristiansen, R., and Larsen, K. M. H. (2003). The Iceland-Faroe inflow of Atlantic water to the Nordic Seas. *Prog. Oceanogr.* 59, 443–474. doi: 10.1016/j.pocean.2003.10.003

Hátún, H., Chafik, L., and Larsen, K. M. (in prep). *The Norwegian Sea Gyre*.

Hátún, H., Hansen, B., and Haugan, P. (2004). Using an "Inverse Dynamic Method" to determine temperature and salinity fields from ADCP measurement. *J. Atmos. Ocean. Technol.* 21, 527–534.

Hays, G. C. (2003). A review of the adaptive significance and ecosystem consequences of zooplankton diel vertical migration. *Hydrobiologia* 503, 163–170. doi: 10.1023/b:hydr.0000008476.23617.b0

Heywood, K. J. (1996). Diel vertical migration of zooplankton in the northeast Atlantic. *J. Plankton Res.* 18, 163–184. doi: 10.1093/plankt/18.2.163

Hirche, H.-J., Brey, T., and Niehoff, B. (2001). A high-frequency time series at Ocean Weather Ship Station M (Norwegian Sea): population dynamics of *Calanus finmarchicus*. *Mar. Ecol. Prog. Ser.* 219, 205–219. doi: 10.3354/meps219205

Hovekamp, S. (1989). Avoidance of nets by *Euphausia pacifica* in Dabob Bay. *J. Plankton Res.* 11, 907–924. doi: 10.1093/plankt/11.5.907

Huse, G., Utne, K. R., and Fernö, A. (2012). Vertical distribution of herring and blue whiting in the Norwegian Sea. *Mar. Biol. Res.* 8, 488–501. doi: 10.1080/17451000.2011.639779

ICES (2020). *Working Group of International Pelagic Surveys (WGIPS)*. Dublin: ICES.

Jónasdóttir, S. H., Visser, A. W., Richardson, K., and Heath, M. R. (2015). Seasonal copepod lipid pump promotes carbon sequestration in the deep North Atlantic. *Proc. Natl. Acad. Sci. U.S.A.* 112, 12122–12126. doi: 10.1073/pnas.1512110112

Klevjer, T. A., Irigoien, X., Røstad, A., Fraile-Nuez, E., Benítez-Barrios, V. M., and Kaartvedt, S. (2016). Large scale patterns in vertical distribution and behavior of mesopelagic scattering layers. *Sci. Rep.* 6:19873. doi: 10.1038/srep19873

Knutsen, T., and Serigstad, B. (2001). *Potential Implications on the Pelagic Fish and Zooplankton Community of Artificially Induced Deep-Water Release of Oil and Gas During DeepSpill_2000 – An Innovative Approach. Fisken og Havet 14, 1-37*. Available online at: http://www.imr.no/filarkiv/2003/08/biology_report.pdf/nb-no (accessed December 15, 2020).

Kristiansen, I., Jónasdóttir, S. H., Gaard, E., Eliasen, S. K., and Hátún, H. (accepted). Seasonal variations in population dynamics of *Calanus finmarchicus* in relation to environmental conditions in the southwestern Norwegian Sea. *Deep Sea Res.*

Lamhauge, S., Jacobsen, J. A., Jákupsstovu, S. H. Í., Valdemarsen, J. W., Sigurdsson, T., Bardarsson, B., et al. (2008). *Fishery and Utilisation of Mesopelagic Fishes and Krill in the North Atlantic*. (Copenhagen: Nordic Minister Council), 1–36.

Lampert, W. (1989). The adaptive significance of diel vertical migration of zooplankton. *Funct. Ecol.* 3, 21–27. doi: 10.2307/2389671

Larsen, K. M. H., Hansen, B., and Svendsen, H. (2008). Faroe Shelf Water. *Cont. Shelf Res.* 28, 1754–1768. doi: 10.1016/j.csr.2008.04.006

Longhurst, A. R., and Harrison, W. G. (1988). Vertical nitrogen flux from the oceanic photic zone by diel migrant zooplankton and nekton. *Deep Sea Res. A Oceanogr. Res. Pap.* 35, 881–889. doi: 10.1016/0198-0149(88)90065-9

Luo, J., Ortner, P. B., Forcucci, D., and Cummings, S. R. (2000). Diel vertical migration of zooplankton and mesopelagic fish in the Arabian Sea. *Deep Sea Res. I Oceanogr. Res. Pap.* 47, 1451–1473. doi: 10.1016/s0967-0645(99)00150-2

Melle, W., Kaartvedt, S., Knutsen, T., Dalpadado, P., and Skjoldal, H. R. (1993). *Acoustic Visualization of Large Scale Macroplankton and Micronekton Distributions Across the Norwegian Shelf and Slope of the Norwegian Sea*. Available online at: http://hdl.handle.net/11250/105194 (accessed December 15, 2020).

Monstad, T. (2004). "Blue Whiting," in *The Norwegian Sea Ecosystem, 263-314*, ed. Skjoldal (Trondheim: Tapir Academic Press), 559.

Mullison, J. (2017). *Backscatter Estimation Using Broadband Acoustic Doppler Current Profilers - Updated. Application Note. 8–13 (Teledyne RD Instruments FSA-031)*. Available online at: http://www.teledynemarine.com/Documents/

Brand%20Support/RD%20INSTRUMENTS/Technical%20Resources/Technical%20Notes/WorkHorse%20-%20ADCP%20Special%20Applications%20and%20Modes/FSA031.pdf (accessed December 15, 2020).

Neilson, J. D., and Perry, R. I. (1990). Diel vertical migrations of marine fishes: An Obligate or Facultative Process? *Adv. Mar. Biol.* 26, 115–168. doi: 10.1016/s0065-2881(08)60200-x

Plueddemann, A. J., and Pinkel, R. (1989). Characterization of the patterns of diel migration using a Doppler sonar. *Deep Sea Res. A Oceanogr. Res. Pap.* 36, 509–530. doi: 10.1016/0198-0149(89)90003-4

Prokopchuk, I., and Sentyabov, E. (2006). Diets of herring, mackerel, and blue whiting in the Norwegian Sea in relation to *Calanus finmarchicus* distribution and temperature conditions. *ICES J. Mar. Sci.* 63, 117–127. doi: 10.1016/j.icesjms.2005.08.005

Proud, R., Cox, M. J., and Brierley, A. S. (2017). Biogeography of the Global Ocean's Mesopelagic Zone. *Curr. Biol.* 27, 113–119. doi: 10.1016/j.cub.2016.11.003

Read, J. F., and Pollard, R. T. (1992). Water masses in the region of the Iceland–Faeroes Front. *J. Phys. Oceanogr.* 22, 1365–1378. doi: 10.1175/1520-0485(1992)022<1365:wmitro>2.0.co;2

Reda, I., and Andreas, A. (2004). Solar position algorithm for solar radiation applications. *Sol. Energy* 76, 577–589. doi: 10.1016/j.solener.2003.12.003

Ringelberg, J. (1995). Changes in light intensity and diel vertical migration: a comparison of marine and freshwater environments. *J. Mar. Biol. Assoc. U.K.* 75, 15–25. doi: 10.1017/s0025315400015162

Roe, H. S. J. (1974). Observations on the diurnal vertical migrations of an oceanic animal community. *Mar. Biol.* 28, 99–113. doi: 10.1007/bf00396301

Salvanes, A. G. V. (2004). "Mesopelagic fish," in *The Norwegian Sea Ecosystem*, eds H. R. Skjoldal, R. Sætre, A. Færnö, O. A. Misund, and I. Røttingen (Trondheim: Tapir Academic Press), 301–314.

Salvanes, A. G. V., and Kristoffersen, J. B. (2001). "Mesopelagic fishes," in *Encyclopaedia of Ocean Sciences*, Vol. 3, eds S. Steele, S. Thorpe, and K. Turekian (San Diego, CA: Academic Press), 1711–1717. doi: 10.1006/rwos.2001.0012

Semper, S., Pickart, R. S., Våge, K., Larsen, K. M. H., Hátún, H., and Hansen, B. (2020). The Iceland-Faroe Slope Jet: a conduit for dense water toward the Faroe Bank Channel overflow. *Nat. Commun.* 11:5390. doi: 10.1038/s41467-020-19049-5

Skjoldal, H. R. (2004). "An introduction to the Norwegian Sea ecosystem. Chap. 2," in *The Norwegian Sea Ecosystem*, ed. H. R. Skjoldal (Trondheim: Tapir Academic Press), 15–32.

Staby, A., Røstad, A., and Kaartvedt, S. (2011). Long-term acoustical observations of the mesopelagic fish *Maurolicus muelleri* reveal novel and varied vertical migration patterns. *Mar. Ecol. Prog. Ser.* 441, 241–255. doi: 10.3354/meps09363

Staby, A., Srisomwong, J., and Rosland, R. (2013). Variation in DVM behavior of juvenile and adult pearlside (*Maurolicus muelleri*) linked to feeding strategies and related predation risk. *Fish. Oceanogr.* 22, 90–101. doi: 10.1111/fog.12012

Stenevik, E. K., Melle, W., Gaard, E., Gislason, A., Broms, C. T., Prokopchuk, I., et al. (2007). Egg production of *Calanus finmarchicus* - a basin-scale study. *Deep Sea Res. II Top. Stud. Oceanogr.* 54, 2672–2685. doi: 10.1016/j.dsr2.2007.08.027

Stensholt, B. K., Aglen, A., Mehl, S., and Stensholt, E. (2002). Vertical density distributions of fish: a balance between environmental and physiological limitation. *ICES J. Mar. Sci.* 59, 679–710. doi: 10.1006/jmsc.2002.1249

Strand, E., Bagøien, E., Edwards, M., Broms, C., and Klevjer, T. (2020). Spatial distributions and seasonality of four Calanus species in the Northeast Atlantic. *Prog. Oceanogr.* 185:102344. doi: 10.1016/j.pocean.2020.102344

Sutton, T. T. (2013). Vertical ecology of the pelagic ocean: classical patterns and new perspectives. *J. Fish Biol.* 83, 1508–1527. doi: 10.1111/jfb.12263

Teledyne RD Instruments (2018). *Workhorse Sentinel, Monitor and Mariner Operation manual, 2018. P/N 957-6150-00 (June 2018)*. Available online at: https://epic.awi.de/id/eprint/40219/1/ADCP_Sentinel_User_Guide.pdf

Torgersen, T., Kaartvedt, S., Melle, W., and Knutsen, T. (1997). Large scale distribution of acoustic scattering layers at the Norwegian continental shelf and the eastern Norwegian Sea. *Sarsia* 82, 87–96. doi: 10.1080/00364827.1997.10413642

Trenkel, V. M., Huse, G., MacKenzie, B. R., Alvarez, P., Arrizabalaga, H., Castonguay, M., et al. (2014). Comparative ecology of widely distributed pelagic fish species in the North Atlantic: implications for modelling climate and fisheries impacts. North Atlantic Ecosystems, the role of climate and anthropogenic forcing on their structure and function. *Prog. Oceanogr.* 129(Part B), 219–243. doi: 10.1016/j.pocean.2014.04.030

Turner, J. T. (2015). Zooplankton fecal pellets, marine snow, phytodetritus and the ocean's biological pump. *Prog. Oceanogr.* 130, 205–248. doi: 10.1016/j.pocean.2014.08.005

Utne, K. R., Huse, G., Ottersen, G., Holst, J. C., Zabavnikov, V., Jacobsen, J. A., et al. (2012). Horizontal distribution and overlap of planktivorous fish stocks in the Norwegian Sea during summers 1995-2006. *Mar. Biol. Res.* 8, 420–441. doi: 10.1080/17451000.2011.640937

Wiborg, K. F. (1955). *Zooplankton in Relation to Hydrography in the Norwegian Sea*. (Bergen: Fiskeridirektoratets havforskningsinstitutt), 1–66.

Zaret, T. M., and Suffern, J. S. (1976). Vertical migration in zooplankton as a predator avoidance mechanism. *Limnol. Oceanogr.* 21, 804–813. doi: 10.4319/lo.1976.21.6.0804

Zhou, M., Nordhausen, W., and Huntley, M. (1994). ADCP measurements of the distribution and abundance of euphausiids near the Antarctic Peninsula in winter. *Deep Sea Res. I Oceanogr. Res. Pap.* 41, 1425–1445. doi: 10.1016/0967-0637(94)90106-6

Conflict of Interest: The authors declare that the research was conducted in the absence of any commercial or financial relationships that could be construed as a potential conflict of interest.